

1 **Suramin inhibits SARS-CoV-2 infection in cell culture by interfering**
2 **with early steps of the replication cycle**

3
4
5
6
7
8
9
10
11
12
13
14
15
16
17
18
19
20
21
22
23
24
25
26
27
28
29
30
31
32
33
34
35
36
37
38
39

Clarisse Salgado Benvindo da Silva^{1*}, Melissa Thaler^{1*}, Ali Tas¹, Natacha S. Ogando¹, Peter J. Bredenbeek¹, Dennis K. Ninaber², Ying Wang², Pieter S. Hiemstra², Eric J. Snijder¹, Martijn J. van Hemert¹

- 40 1. Department of Medical Microbiology, Leiden University Medical Center, Leiden, The
41 Netherlands.
42 2. Department of Pulmonology, Leiden University Medical Center, Leiden, The Netherlands.
43 * These authors contributed equally to this work.

44
45 Corresponding author: Martijn van Hemert, Albinusdreef 2, 2333ZA Leiden, the Netherlands.
46 E-mail: M.J.van_Hemert@lumc.nl

47 **Abstract**

48 The SARS-CoV-2 pandemic that originated from Wuhan, China, in December 2019 has impacted public
49 health, society and economy and the daily lives of billions of people in an unprecedented manner.
50 There are currently no specific registered antiviral drugs to treat or prevent SARS-CoV-2 infections.
51 Therefore, drug repurposing would be the fastest route to provide at least a temporary solution while
52 better, more specific drugs are being developed. Here we demonstrate that the antiparasitic drug
53 suramin inhibits SARS-CoV-2 replication, protecting Vero E6 cells with an EC₅₀ of ~20 μM, which is well
54 below the maximum attainable level in human serum. Suramin also decreased the viral load by 2-3
55 logs when Vero E6 cells or cells of a human lung epithelial cell line (Calu-3) were treated. Time of
56 addition and plaque reduction assays showed that suramin acts on early steps of the replication cycle,
57 possibly preventing entry of the virus. In a primary human airway epithelial cell culture model, suramin
58 also inhibited the progression of infection. The results of our preclinical study warrant further
59 investigation and suggest it is worth evaluating whether suramin provides any benefit for COVID-19
60 patients, which obviously requires well-designed, properly controlled randomized clinical trials.

61 Introduction

62 In December 2019, local health authorities reported an increasing number of pneumonia cases, rapidly
63 spreading across the city of Wuhan, Hubei province, in China (1). Further analysis showed that the
64 causative agent of this disease was SARS-coronavirus-2 (SARS-CoV-2), which is a member of the
65 betacoronavirus genus within the coronavirus family and shares roughly 80% of genetic identity with
66 SARS-CoV (2, 3). Since then, SARS-CoV-2 has spread to 113 countries, leading to a coronavirus
67 pandemic of unprecedented magnitude, with more than 3.5 million confirmed cases globally and more
68 than 240,000 casualties reported by WHO on May 5th, 2020 (4).

69 Coronaviruses are enveloped viruses, that possess extraordinarily large (26 to 32 kb) positive-strand
70 RNA genomes (5). SARS-CoV-2 infection often causes only mild disease, but can also lead to clinical
71 manifestations such as high fever, cough, dyspnea, myalgia and headache. Although the majority of
72 cases may be asymptomatic or present mild symptoms with good recovery, some patients develop
73 more severe outcomes, such as severe pneumonia, respiratory failure, multiple organ failure or death
74 (6).

75 Due to the urgency of the situation, the lack of approved specific antiviral therapy against
76 coronaviruses and the time it takes to develop the latter through regular preclinical and clinical
77 research, there is great interest in repurposing already approved drugs. This would be a fast track to
78 apply candidate therapeutic agents as antivirals to combat SARS-CoV-2 infection, which can be used
79 to fight the virus while better and more specific antivirals are being developed.

80 Drugs like ribavirin, remdesivir, favipiravir and the anti-malarial therapeutic chloroquine showed
81 promise in cell culture and some also appeared to show (modest) effects in early trials in humans,
82 which were not always conducted with the most optimal design (7). However, except for remdesivir
83 (8) more recent (and more appropriately conducted) clinical trials suggest that none of these drugs
84 provide substantial benefit in patients and that they should be used with caution due to their potential
85 side-effects. Therefore, it appears that options to inhibit SARS-CoV-2 infection are limited and mainly
86 supportive care and treatments that target the immune system and inflammatory responses can be
87 provided to patients. This stresses the urgency of evaluating additional approved drugs as candidates
88 for use as antiviral therapy against this pathogen.

89 We now provide evidence showing that suramin can be considered as drug candidate that deserves
90 further assessment, as we found the compound to exhibit antiviral activity against SARS-CoV-2 in
91 relevant cell culture models at concentrations that can be easily reached in human serum. Suramin is
92 an anti-parasitic drug that is used to treat sleeping sickness caused by trypanosomes. It is a
93 symmetrical polysulfonated compound that was synthesized for the first time around 1916 (9). Later
94 we and many others have shown that suramin also has broad-spectrum antiviral effects, as it inhibits
95 HIV (10), hepatitis C virus (11), herpes simplex type-1 virus (12), Zika virus (13), dengue virus (14),
96 chikungunya virus (15), and others.

97 In the present study, we show that suramin also exhibits antiviral activity against SARS-CoV-2 in cell
98 culture, most likely by inhibiting viral entry. The compound had an EC₅₀ of 20 µM in Vero E6 cells and
99 showed a more than 2 log viral load reduction when infected human Calu-3 airway epithelial cells
100 were treated. Finally, suramin reduced SARS-CoV-2 progression of infection in well-differentiated
101 primary human airway epithelial cells cultured at the physiological air-liquid interface. It is important
102 to stress that these results should not be directly translated to efficacy against SARS-CoV-2 in humans
103 and guarantee no benefit to the patient yet. However, our results make suramin an interesting
104 candidate to further evaluate in in-depth pre-clinical studies (e.g. into formulation, mode of
105 administration, pharmacokinetics and in other *ex vivo* models) and suggest suramin could be explored
106 in carefully performed and properly controlled clinical trials for the treatment of COVID-19 patients.

107
108
109
110
111

112 **Material and Methods**

113 **Cell lines, virus and compound**

114 Vero E6 cells were maintained in Dulbecco's modified Eagle's medium (DMEM; Lonza), supplemented
115 with 8% fetal calf serum (FCS; Bodinco), 2 mM L-glutamine, 100 IU/ml of penicillin and 100 µg/ml of
116 streptomycin (Sigma-Aldrich). The human lung epithelial cell line Calu-3 2B4 (referred to as Calu-3
117 cells) was maintained as described (16). Primary human airway epithelial (HAE) cell cultures were
118 established at the Leiden University Medical Center (LUMC; Department of Pulmonology) and their
119 culture and infection are described below. All cell cultures were maintained at 37°C in an atmosphere
120 of 5% CO₂ and 95%–99% humidity. Infections were performed in Eagle's minimal essential medium
121 (EMEM; Lonza) with 25 mM HEPES (Lonza), further supplemented with 2% FCS, L-glutamine (Sigma-
122 Aldrich), and antibiotics.

123 The clinical isolate SARS-CoV-2/Leiden-002 was isolated from a nasopharyngeal sample at LUMC and
124 its sequence and characterization will be described elsewhere (manuscript in preparation). SARS-CoV-
125 2/Leiden-002 was passaged twice in Vero E6 cells and virus titers were determined by plaque assay as
126 described before (17). Working stocks yielded titers of 5 x 10⁶ plaque forming units (PFU)/ml. All
127 experiments with infectious SARS-CoV-2 were performed in a biosafety level 3 facility at the LUMC.
128 Suramin was purchased from Sigma-Aldrich and was dissolved in milliQ and stored at -20°C. Addition
129 of compound to Vero E6 and Calu-3 cells was done in infection medium and in PBS for HAE cultures.

130

131 **Human airway epithelial cell cultures (HAE)**

132 HAE cell cultures were cultured as previously described (18). Briefly, primary human bronchial
133 epithelial cells were isolated from tumour-free resected bronchial tissue from patients undergoing
134 resection surgery for lung cancer at the LUMC. Use of such lung tissue that became available for
135 research within the framework of patient care was in line with the "Human Tissue and Medical
136 Research Code of conduct for responsible use" (2011) (www.federa.org), which describes the opt-out
137 system for coded anonymous further use of such tissue. To achieve mucociliary differentiation, PBEC
138 were cultured at the air-liquid interface (ALI) for 21 days as previously described (18, 19). In brief,
139 expanded HAE cells from 3 donors at passage 2 were combined (3 x 10⁴ cells per donor) and were
140 seeded on 12-well transwell membranes (Corning Costar), which were coated with a mixture of BSA,
141 collagen type 1, and fibronectin. In addition, cells from two individual donors were seeded on separate
142 sets of transwell membranes. BEpiCM-b:DMEM (B/D)-medium (1:1) was used as described
143 (supplemented with 12.5mM HEPES, bronchial epithelial cell growth supplement, antibiotics, 1 nM
144 EC23 (retinoic acid receptor agonist), and 2 mM glutaMAX). After confluence was reached, cells were
145 cultured at the ALI in complete medium with 50 nM EC23 for 21 days. The mucociliary differentiated
146 cultures were characterized by a high trans-epithelial electrical resistance (TEER>500 Ω·cm²), visible
147 cilia beating and mucus production. Before infection, cells were incubated overnight in the BEpiCM-
148 b/DMEM 1:1 medium mixture from which EGF, BPE, BSA and hydrocortisone were omitted and that
149 did contain antibiotics (starvation medium).

150

151 **RNA isolation and quantitative RT-PCR (RT-qPCR)**

152 RNA was isolated from cell culture supernatants and cell lysates using the TriPure Isolation Reagent
153 (Sigma-Aldrich). Equine arteritis virus (EAV) in AVL lysis buffer (Qiagen) was spiked into the reagent as
154 internal control for extracellular RNA samples. The cellular housekeeping gene PGK-1 served as control
155 for intracellular RNA. Primers and probes for EAV and PGK1 and the normalization procedure were
156 described before (20). Viral RNA was quantified by RT-qPCR using the TaqMan™ Fast Virus 1-Step
157 Master Mix (Thermo Fisher Scientific). Primers and probes were based on (21) but with modifications
158 resulting in the following primer and probe sequences: SARS-CoV-2 N-Gene Fwd-
159 CACATTGGCACCCGCAATC, Rev-GAGGAACGAGAAGAGGCTTG and Probe YakYel-
160 ACTTCCTCAAGGAACAACATTGCCA-BHQ1; RdRp-Gene Fwd-GTGARATGGTCATGTGTGGCGG, Rev-
161 CARATGTTAAASACTATTAGCATA and Probe FAM- CCAGGTGGAACMTCATCMGGWGATGC-BHQ1. A
162 standard curve of 10-fold serial dilutions of a T7 RNA polymerase-generated *in vitro* transcript

163 containing the RT-qPCR target sequences was used for absolute quantification. A RT-qPCR program of
164 5 min at 50 °C and 20 s at 95 °C, followed by 45 cycles of 5 s at 95 °C and 30 s at 60 °C, was performed
165 on a CFX384 Touch™ Real-Time PCR Detection System (Bio-Rad).

166

167 **Cytopathic effect (CPE) reduction assay**

168 CPE reduction assays were performed as described (22). Briefly, Vero E6 cells were seeded in 96-well
169 cell culture plates at a density of 10^4 cells per well. Cells were incubated with 1.7-fold serial dilutions
170 of suramin starting from a concentration of 120 μ M. Subsequently, cells were either mock-infected
171 (analysis of cytotoxicity of the compound) or were infected with 300 PFU of virus per well (MOI of
172 0.015) in a total volume of 150 μ l of medium. Cell viability was assessed three days post-infection by
173 MTS assay using the CellTiter 96® Aqueous Non-Radioactive Cell Proliferation kit (Promega) and
174 absorption was measured at 495 nm with an EnVision Multilabel Plate Reader (PerkinElmer). The 50%
175 effective concentration (EC_{50}), required to inhibit virus-induced cell death by 50%, and the 50%
176 cytotoxic concentration (CC_{50}), that reduces the viability of uninfected cells to 50% of that of untreated
177 control cells, were determined using non-linear regression with GraphPad Prism v8.0.

178

179 **Viral load reduction assays**

180 Cells were seeded in 96-well cell culture plates at a density of 10^4 (Vero E6) or 6×10^4 (Calu-3) cells per
181 well in 100 μ l culture medium. As control to determine the amount of residual virus after removal of
182 the inoculum and washing, cells in some wells were killed with 70% Ethanol (followed by washing with
183 PBS). Vero E6 and Calu-3 cells were incubated with 2-fold serial dilutions of a starting concentration
184 of 200 μ M of suramin and subsequently infected with 2×10^4 PFU of SARS-CoV-2 (MOI of 1 on Vero E6
185 cells). For analysis of viral RNA, supernatant was harvested from Vero E6 cells at 16 h.p.i and from
186 Calu-3 cells at 21 h.p.i. Intracellular RNA was collected by lysing the cells in 150 μ l Tripure reagent.
187 Analysis of viral progeny in supernatant from Calu-3 cells was performed by plaque assay on Vero E6
188 cells (17). Potential cytotoxicity of the compound was tested in parallel on uninfected cells using the
189 MTS assay (Promega) as described for the CPE reduction assay.

190

191 **Entry inhibition plaque reduction assay**

192 A day before infection Vero E6 cells were seeded in 6-well cell culture plates at a density of 3.5×10^5
193 cells per well in 2 ml medium. 10^{-2} to 10^{-5} -fold serial dilutions of a SARS-COV-2 stock were prepared in
194 medium containing 100, 50, 25, 12.5, 6.25 or 0 μ M suramin. These were used as inoculum to infect
195 the Vero E6 cells in 6-well clusters. After 1 h at 37°C, the inoculum was removed and cells were
196 incubated in Avicel-containing overlay medium without suramin for 3 days, after which they were
197 fixed with 3.7% formaldehyde, stained with crystal violet and plaques were counted (17).

198

199 **Time of addition assay**

200 Vero E6 cells were seeded in 24-well clusters at a density of 6×10^4 cells per well. The next day cells
201 were treated with 100 μ M suramin during the time intervals indicated in Fig. 3 and they were infected
202 at an MOI of 1. Supernatant was harvested at 10 h.p.i. for quantification of viral RNA by RT-qPCR.

203

204 **Infection and suramin treatment of HAE cells**

205 The apical sides of HAE cell cultures were washed 3 times with 200 μ l PBS for 10 min at 37°C on the
206 day before infection to remove excess mucus. Washing was repeated once before cells were infected
207 on the apical side with 3×10^4 PFU SARS-CoV-2 (estimated MOI of 0.1) in 200 μ l of PBS. The apical side
208 was treated with 100 μ M suramin in 50 μ l of PBS at 12 and 24 h.p.i (after first collecting a 200 μ l PBS
209 wash to determine viral load). Control wells were treated with 50 μ l of PBS. The experiment was done
210 in triplicate, with one insert (transwell) containing a mix of cells from 3 donors and two 'single donor'
211 inserts seeded with cells from two different donors. Supernatants were collected from infected PBS-
212 treated cells and infected suramin-treated cells at 12, 24 and 48 h.p.i, by incubating the apical side
213 with 200 μ l PBS for 10 min at 37°C and collecting it. This supernatant was used for quantification of

214 viral RNA by RT-qPCR and viral load (infectivity) by plaque assay on Vero E6 cells. At each timepoint
215 cell lysates were collected from inserts by adding 750 μ l Tripure reagent. Assessment of potential
216 cytotoxicity of the 48h suramin treatment, compared to PBS treatment, was done with uninfected
217 cells by MTS assay (Promega) and LDH Assay (CytoTox 96[®] Non-Radioactive Cytotoxicity Assay,
218 Promega) according to the manufacturer's instructions.

219
220

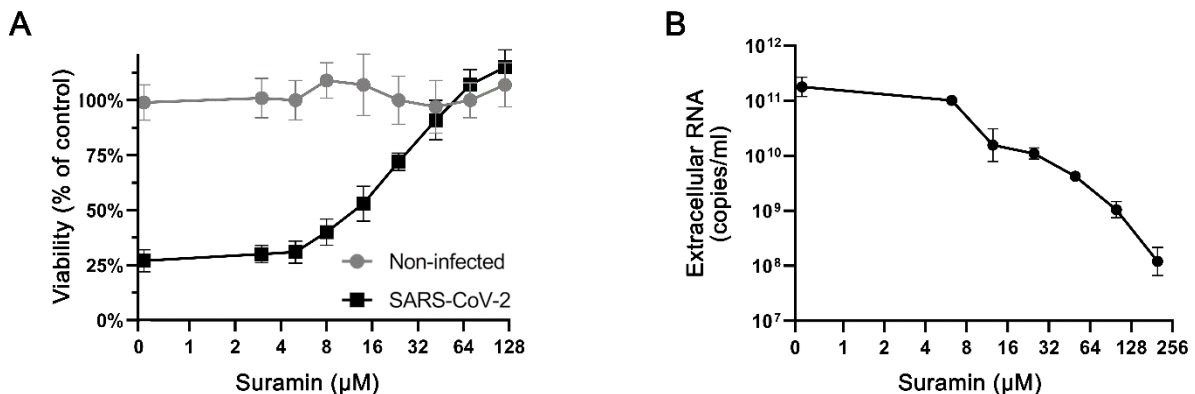
221 Results

222 Suramin inhibits SARS-CoV-2 replication in Vero E6 cells

223 To determine if suramin could protect cells from SARS-CoV-2 infection and to evaluate its toxicity,
224 Vero E6 cells were infected with SARS-CoV-2 and treated with serial dilutions of suramin in a CPE
225 reduction assay. Suramin protected infected cells from SARS-CoV-2-induced cell death in a dose-
226 dependent manner, with an EC₅₀ of $20 \pm 2,7 \mu$ M (Fig. 1A). In parallel, non-infected cells were treated
227 with the same concentrations of suramin in order to assess the compound's toxicity. No toxicity was
228 observed over the range of concentrations that was used in these antiviral assays. Only at 5 mM cell
229 viability dropped to 67%, resulting in a CC₅₀ > 5 mM (15). Therefore, suramin inhibits SARS-CoV-2 with
230 a selectivity index (SI) higher than 250.

231 To more directly measure the inhibition of viral replication by suramin, viral load reduction assays
232 were performed. Vero E6 cells were infected with SARS-CoV-2 at an MOI of 1 and they were treated
233 with increasing concentrations of suramin. At 16 h.p.i., supernatant was harvested to determine the
234 viral load by quantifying the levels of extracellular viral RNA by RT-qPCR (Fig 1B). The supernatant of
235 untreated infected cells contained 10^{11} copies/ml of viral RNA. RT-qPCR revealed that the RNA levels
236 decreased upon suramin treatment in a dose-dependent manner, showing a 3-log reduction at the
237 highest concentration tested (200 μ M) (Fig. 1B). Together, these results indicated that suramin
238 protects Vero E6 cells from the SARS-CoV-2-induced cytopathic effect and that it reduces the viral load
239 in these cells.

240
241



242
243

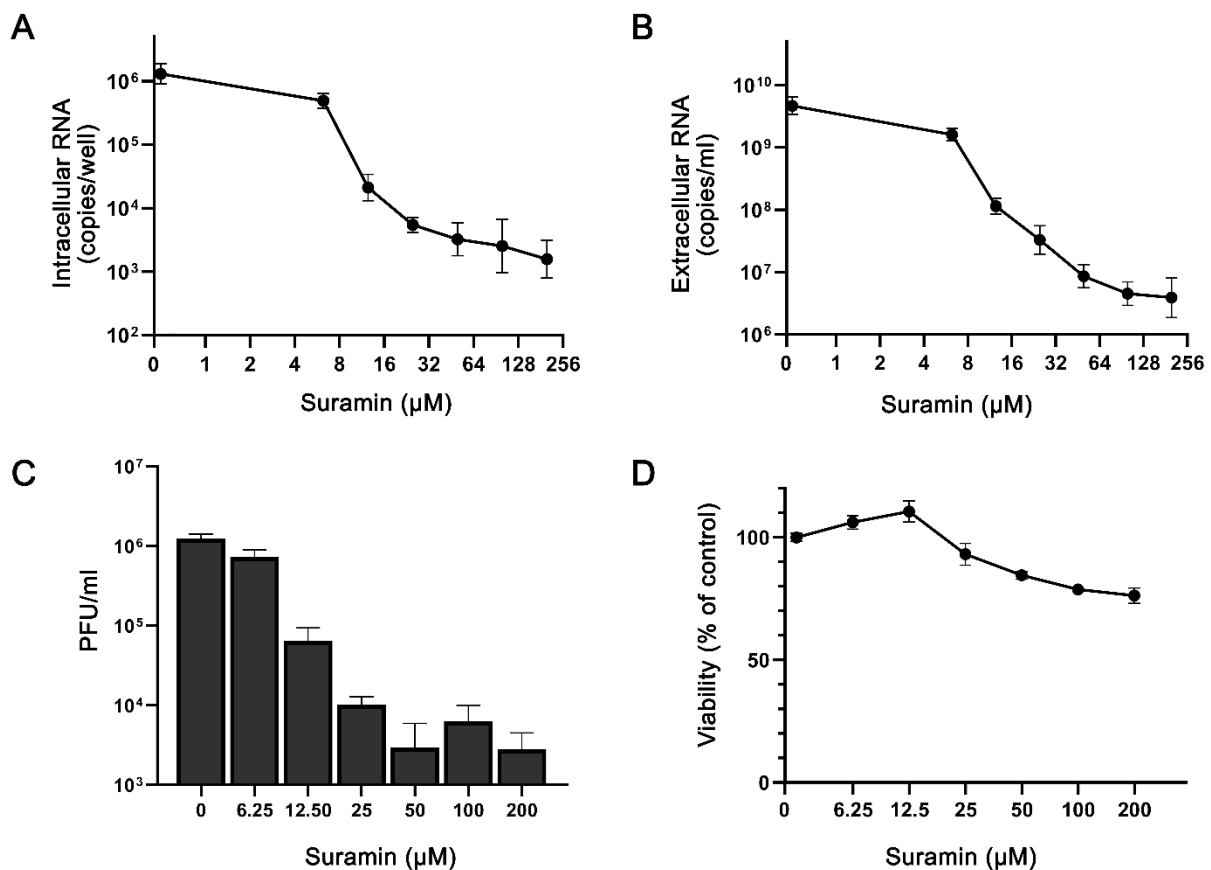
244 **Figure 1. Suramin inhibits SARS-CoV-2 replication in Vero E6 cells.** (A) CPE reduction assay. Vero E6
245 cells were infected with SARS-CoV-2 at an MOI of 0.015 and were treated with 1.7-fold serial dilutions
246 of suramin. Viability was measured by MTS assay at 3 days post infection. The viability of non-infected
247 suramin-treated cells was measured in parallel to assess toxicity (3 independent experiments
248 performed in quadruplicate). (B) Viral load reduction assay. Vero E6 cells were infected at an MOI of 1,
249 followed by treatment with different concentrations of suramin. After 16 hours, supernatants were
250 harvested and the viral load was determined by quantification of extracellular SARS-CoV-2 RNA by an
251 internally controlled multiplex RT-qPCR (n=3).

252
253

254 Suramin reduces the viral RNA and infectious virus load in cultured human lung epithelial cells

255 To assess the antiviral effect of suramin in a more relevant model, human lung epithelial cells (Calu-3)
256 were infected with 2×10^4 PFU of SARS-CoV-2 in the presence of 0-200 μM suramin for 1h. After
257 removal of the inoculum and washing of the cells, incubation was continued in medium with suramin
258 (0-200 μM) for 20 hours. At 21 h.p.i., RNA was isolated from cells and supernatant and the viral titer
259 in the supernatant was determined by plaque assay. We observed a strong dose-dependent reduction
260 in intracellular (Fig. 2A) and extracellular (Fig. 2B) viral RNA levels in suramin-treated samples. At 200
261 μM the extracellular viral RNA levels showed a 3-log reduction, while intracellular viral RNA levels
262 decreased by 2-log. Figures 2A and 2B show the results of RT-qPCR reactions targeting the RNA-
263 dependent RNA polymerase coding region, but similar reductions in copy numbers were observed
264 with RT-qPCR reactions targeting the SARS-CoV-2 N protein gene (also detects subgenomic RNA),
265 although in that case absolute copy numbers -as expected- were higher than for genomic RNA (data
266 not shown). Plaque assays confirmed that treatment with 200 μM suramin led to an almost 3-log drop
267 in infectious progeny titers from infected-Calu-3 cells (Fig. 2C).
268 Cytotoxicity assays performed in parallel in non-infected Calu-3 cells showed that suramin was slightly
269 more toxic to these cells than to Vero E6 cells, although cell viability remained above 80% even at the
270 highest dose tested (Fig. 2D). Together these results suggest that suramin is a potent SARS-CoV-2
271 inhibitor with high selectivity, also in human lung cells.

272
273



274
275
276
277
278
279
280
281

282 **Figure 2. Suramin decreases levels of intra- and extracellular viral RNA and infectious progeny in**
283 **infected Calu-3 cells.** Calu-3 cells were infected with SARS-CoV-2, followed by treatment with 0-200
284 μM suramin. (A) Intracellular viral RNA copy numbers at 21 h.p.i., determined by internally controlled
285 multiplex RT-qPCR targeting the SARS-CoV-2 RdRp coding region and using the housekeeping gene
286 PGK1 for normalization. (B) Extracellular viral RNA levels at 21 h.p.i., quantified by RT-qPCR. (C) Viral
287 load in the supernatant at 21 h.p.i. as determined by plaque assay on Vero E6 cells. (D) Viability of
288 uninfected Calu-3 cells treated with various concentrations of suramin measured by MTS assay in
289 parallel to the infection ($n=3$).

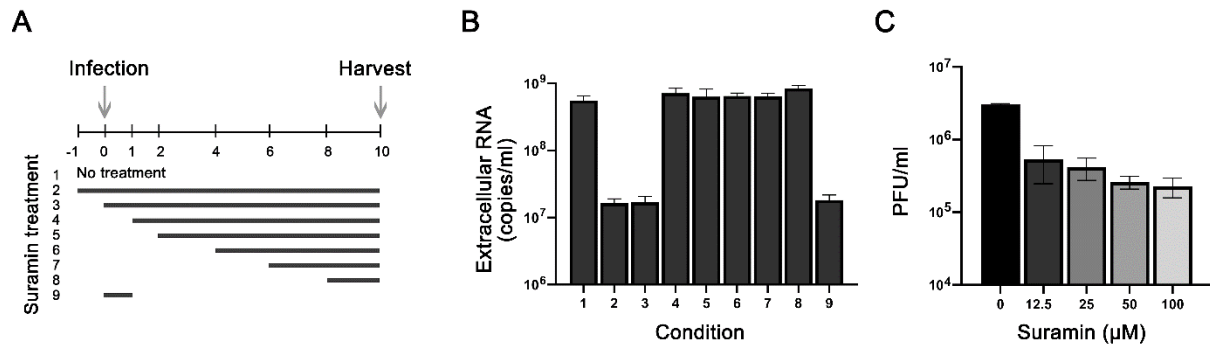
290
291
292

293 **Suramin acts on the early steps of viral replication**

294 To determine which step of viral replication is affected by suramin, we performed a time-of-addition
295 assay. Cells were infected with SARS-CoV-2 (MOI 1) and treated with 100 μM of suramin over different
296 time intervals, as schematically depicted in Figure 3A. Treatment was initiated 1 hour before infection
297 or at 0, 1, 2, 4, 6 or 8 h.p.i., and suramin remained present until 10 h.p.i., when supernatants were
298 harvested to determine viral load by RT-qPCR targeting the RdRp coding region. In one sample suramin
299 was only present for 60 min during the time of infection. After 1 hour, virus inoculum was removed
300 and cells were washed three times with PBS, followed by incubation in medium with or without
301 suramin. At 10 h.p.i., supernatant was collected to evaluate the levels of viral RNA (Fig. 3B). When
302 suramin treatment was initiated 1 hour before (-1h) or at the time of infection (0h) a 2-log reduction
303 in viral RNA levels was observed. Treatments that started later than 1 hour post infection did not
304 inhibit viral replication, as viral RNA levels similar to the non-treated control were observed.
305 Treatment only during the infection (0-1h) resulted in the same 2-log reduction in viral RNA load as
306 the 0-10h treatment, indicating that suramin inhibits an early step of the replication cycle, likely viral
307 entry.

308 To confirm suramin's inhibitory effect on entry, we performed a plaque reduction assay, by infecting
309 Vero E6 cells with serial dilutions of SARS-CoV-2 in the presence of increasing concentrations of
310 suramin, which was only present during the one hour of infection. After infection, cells were washed
311 3 times with PBS and were incubated with overlay medium without suramin. After 3 days, cells were
312 fixed, stained and plaques were counted. Suramin caused a dose-dependent reduction in the number
313 of plaques and even at the lowest suramin concentration (12.5 μM) titers were already reduced by
314 almost one log (Fig. 3C). These results suggest that suramin inhibits SARS-CoV-2 entry.

315



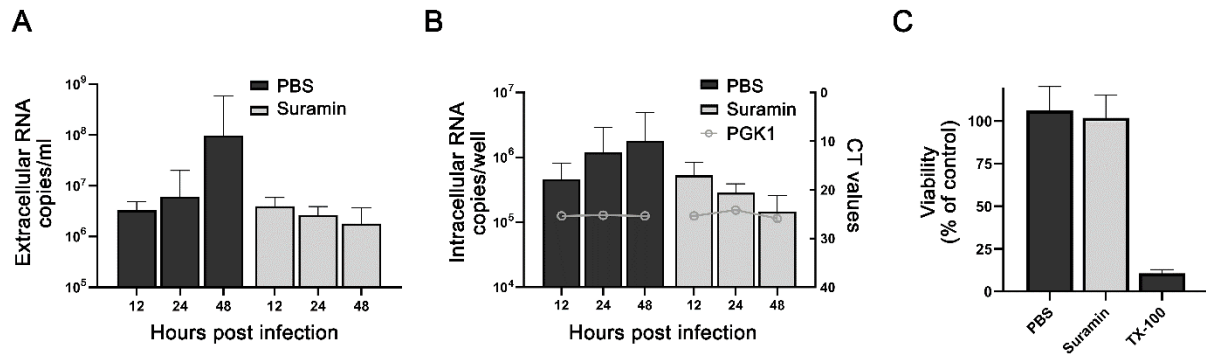
316
317
318
319
320
321
322
323
324
325

Figure 3. Suramin inhibits the early steps of SARS-CoV-2 replication. (A) Schematic representation of the time-of-addition experiment and the different treatment intervals. (B) At 10 h.p.i. supernatant was harvested and extracellular viral RNA levels were determined by RT-qPCR. (C) Vero E6 cells were infected with SARS-CoV-2 in the presence of various concentrations of suramin. Suramin was only present during the one hour of infection and after 1 hour, cells were incubated in overlay medium without suramin. After three days, cells were fixed, stained and plaques were counted. (n=3).

326 Suramin inhibits SARS-CoV-2 replication in a primary human epithelial airway cell infection model

327 Primary human airway epithelial cell cultures (HAE) mimic the morphological and physiological
328 features of the human conducting airway, arguably being the most relevant *ex vivo* model for human
329 coronavirus research (23-25). For that reason, we decided to also evaluate the antiviral effect of
330 suramin in this model. HAE were differentiated by culture at the air-liquid interface to achieve
331 mucociliary differentiation, and were infected for one hour with 30,000 PFU of SARS-CoV-2 (estimated
332 MOI of 0.1 based on the number of cells present on an insert), followed by washing with PBS. At 12
333 and 24 h.p.i., the cultures were treated on the apical side with either 50 μ l of 100 μ M suramin or 50
334 μ l PBS. The HAE apical side was washed with PBS for 10 minutes at 37°C, and this supernatant was
335 harvested at 12, 24 and 48 h.p.i. to analyze the viral load by RT-qPCR. RNA was also isolated from cells
336 to quantify the levels of intracellular viral RNA and the housekeeping gene PGK1. RT-qPCR analysis of
337 extracellular viral RNA levels showed that after infection approximately 10⁷ copies/ml of viral RNA
338 remained at 1 h.p.i.. The viral load in the supernatant did not increase significantly at 12 and 24 h.p.i.
339 in untreated cells, while at 48h a more than 1 log increase in viral RNA copies was observed. This is
340 indicative of (very modest) viral replication in PBS-treated cells. The cultures that were treated with
341 suramin displayed no increase in viral load in the supernatant, but rather even a slight decrease in
342 copy numbers, suggesting viral replication did not progress in treated cells. At 48 h.p.i. the supernatant
343 of suramin-treated cells showed 2-log lower SARS-CoV-2 released genome copy numbers than PBS-
344 treated control cells (Fig. 4A). The levels of intracellular viral RNA displayed the same trend, with a
345 decrease in viral RNA in suramin-treated samples compared to an increase in viral RNA in PBS-treated
346 samples (Fig. 4B). A 1-log difference, from 10⁶ to 10⁵ copies per transwell was observed at 48 h.p.i.
347 between suramin- and PBS-treated cells (Fig. 4B). The levels of the housekeeping gene, PGK1 remained
348 stable in all samples, suggesting the reduction in viral RNA copies was not due to cell death. Moreover,
349 cell viability measured by MTS assay (Fig. 4C) and LDH assay (data not shown), suggested suramin
350 treatment (compared to PBS treatment) had no measurable cytotoxic effect on HAE cells. To
351 determine the effect of suramin on infectious progeny released by HAE cells, we performed a plaque
352 assay with the harvested supernatant. At 24 h.p.i., a modest difference was observed between the
353 infectious progeny released by PBS (3.3 x 10³ PFU/ml) and suramin-treated cells (4.4 x 10² PFU/ml).
354 At 48 h.p.i., the supernatant of PBS-treated cells contained over 10⁴ PFU/ml, while no infectious virus
355 was found in suramin-treated samples (Limit of detection 100 PFU/ml). This suggests that suramin
356 reduces the progression of infection in a HAE culture infection model.

357



358
359

360 **Figure 4. Suramin inhibits progression of SARS-CoV-2 infection in primary human airway epithelial**
361 **cells.** HAE cells were infected with 30,000 PFU of SARS-CoV-2 (estimated MOI of 0.1) and they were
362 treated with 50 μ l PBS or 50 μ l of 100 μ M suramin at 12 h.p.i. and 24 h.p.i.. (A) Levels of extracellular
363 viral RNA were determined by RT-qPCR at 12, 24, and 48 h.p.i. (n=3). (B) Intracellular viral RNA levels
364 were determined by RT-qPCR with an internally controlled multiplex (bars, left axis). Levels of the
365 housekeeping gene PGK1 were analyzed to check for signs of cell death (gray lines, right axis). (C)
366 Viability of suramin-treated cells evaluated by MTS assay, using treatment with 0.1% Triton X-100 as
367 a positive control for cell toxicity (n=6).

368
369
370

371 Discussion

372 The emergence of SARS-CoV-2 and its enormous impact on public health, society, economy and the
373 lives of billions around the globe has prompted a multitude of efforts to develop vaccines and
374 antivirals. Due to the lengthy development process of new and specific antivirals, there is a particular
375 interest in repurposing existing drugs for treatment of the COVID-19 disease. This could provide a
376 temporary solution, while better and more specific drugs are being developed. Several small-molecule
377 compounds like chloroquine, hydroxychloroquine, favipiravir or remdesivir have been showing some
378 efficacy against SARS-CoV-2 *in vitro* (26). However, despite promising results in preclinical studies,
379 recent clinical trials (27, 28) suggested that these compounds, with the exception of remdesivir (8), do
380 not provide much benefit to COVID-19 patients and could actually be dangerous due to possible side-
381 effects. This leaves us currently empty-handed and in search for other approved drugs that might be
382 repurposed. As an already approved antiparasitic drug, suramin would be one of the candidates for
383 fast development of a treatment for COVID-19. Antiviral activity of suramin against RNA viruses was
384 reported earlier by us and several other groups (15, 29-31) and the compound was and is also being
385 evaluated in several clinical trials for other diseases, providing some evidence for its safety for
386 therapeutic use. However, suramin can also cause several side-effects, which caused previous HIV
387 trials with seriously ill patients to halt (32) and therefore caution is advised and it is crucial to conduct
388 well controlled randomized trials, before any conclusions on possible benefits for COVID-19 patients
389 can be drawn. Thus far, no studies have reported about a potential antiviral effect of suramin against
390 coronaviruses.

391 In this study we assessed the antiviral activity of suramin against the newly emerged SARS-CoV-2.
392 Suramin offered full protection against SARS-CoV-2-induced cell death in Vero E6 cells and inhibited
393 the virus with an EC₅₀ of 20 μ M and a SI of >250 (Fig. 1). Suramin treatment of infected Vero E6 cells
394 led to a reduction in extracellular viral RNA levels of up to 3 log. The highest concentration of
395 compound that was used proved harmless to the cells and also previously cytotoxicity was only
396 observed above 5 mM (15). Suramin also displayed antiviral efficacy in a human lung epithelial cell
397 line and we observed a >2 log reduction in infectious virus progeny in suramin-treated cells.

398 Suramin was previously described to have the potential to inhibit several stages of virus replication by
399 acting on different targets (15, 33). To assess which step in the SARS-CoV-2 replication cycle is affected
400 by suramin treatment, we performed a time-of-addition assay. We observed that pre-treatment with
401 suramin as well as addition during the first hour of infection resulted in a marked decrease of viral
402 RNA in the supernatant, while treatments initiated after the first hour of infection showed no
403 significant effect on virus replication, suggesting that suramin inhibits binding or entry. In addition,
404 SARS-CoV-2 infectivity was decreased in plaque assays, when suramin was present only in the
405 inoculum during infection, concordant with an effect on the early stages of infection (Fig. 3). This is in
406 agreement with other studies that also reported on the inhibition of virus binding or entry by suramin
407 (15, 30, 34). Our data suggest that the antiviral effect of suramin is primarily due to inhibition of
408 binding and/or fusion.

409 Finally we evaluated the effect of suramin in a more relevant model of differentiated primary human
410 airway epithelial (HAE) cells cultured and infected at the physiologically relevant air-liquid interface.
411 We infected these cells with a relatively low dose of virus (estimated MOI of 0.1) and treated them
412 with suramin by applying a 50 μ l volume of 100 μ M of suramin on the apical side at 12 and 24 h.p.i.
413 This would allow us to follow spread of the viral infection and assess whether suramin is able to block
414 progression of infection in this 'treatment model'. HAE cell cultures are a composition of highly
415 differentiated cells mainly containing basal, goblet, club and ciliated cells, hence representing an air-
416 liquid interface that is mimicking the lung airway epithelium (35, 36). In a recent study, it was shown
417 that SARS-CoV-2, like SARS-CoV, uses human angiotensin-converting enzyme 2 (ACE2) receptors for
418 attachment in these human airway cells. Blocking of the host protease TMPRSS2, which is important
419 for priming the fusion activity of the spike protein, also inhibited infection in lung cells (37). To address
420 the variation of these proteins and the diversity of primary human airway cells within patients, we
421 made use of HAE cultures that were obtained from different donors. Notably, we could observe
422 differences in the susceptibility of cultures from different donors, in which HAE cultures from mixed
423 donors showed higher titers. HAE cultures might have varying susceptibility to infection, possibly
424 caused by a difference in cell differentiation and composition (38).

425 Administration of 100 μ M of suramin on the apical side of the HAE cells did not appear to cause
426 cytotoxic effects in our study (Fig. 4). In our HAE model for progression of SARS-CoV-2 infection, we
427 infected cells at a low MOI and observed a modest (~200-fold) increase in viral load by 48 h.p.i. in PBS-
428 treated cultures. Although the increase in viral load was rather modest in control cells, we found no
429 evidence for progression of the infection in suramin-treated cultures, as indicated by SARS-CoV-2 RNA
430 levels that remained equal to that at 1 h.p.i. or even decreased over time. Moreover, the infectious
431 progeny titer increased over time in PBS-treated HAE cultures and reached over 10^4 PFU/ml by 48
432 h.p.i, while in suramin-treated HAE cells, infectious progeny showed a modest increase at 24 h.p.i. (10
433 fold lower than PBS-treated cells) and dropped to undetectable levels at 48 h.p.i. Since suramin-
434 containing samples needed to be diluted by a 100-fold to exclude interference with the plaque assay,
435 the limit of detection would be 100 pfu/ml. Even with this limit of detection, the supernatant collected
436 from suramin-treated HAE cells contains at least 100 times less virus than that from PBS-treated cells.
437 Much higher titers were obtained with HAE cultures from mixed donors than from single donors, but
438 the inhibitory effect of suramin was also observed with single donor cultures. Overall, despite the
439 modest level of infection in control cells, our results suggest that also in the HAE infection model,
440 suramin has an inhibitory effect on progression of the SARS-CoV-2 infection.

441 Our study demonstrates that suramin inhibits SARS-CoV-2 replication in various cell culture models
442 and at clinically achievable concentrations (after IV administration serum levels of >10x the EC₅₀ could
443 be achieved). Due to its mode of action (inhibition of entry) treatment of patients with suramin might
444 require administration at an early stage, although it might also prevent spread of the virus in the lungs
445 of already symptomatic patients or could prevent spread from respiratory tract to other organs. It
446 might possibly even be used to prevent virus spreading in the nasopharynx, which appears to be the
447 first site of infection (39-41). Standard treatment with suramin is done by intravenous administration,
448 which would also be an option for seriously ill COVID-19 patients that are in intensive care, but is not

449 ideal for other patients. As a negatively charged compound, suramin binds to various proteins and is
450 poorly taken up by diffusion across the cell membrane, although it can be taken up by endocytosis
451 (33). This poor uptake of suramin into cells might not necessarily be a problem for the efficacy against
452 SARS-CoV-2, as it is expected to block the virus systemically and in the extracellular environment.
453 Hypothetically, suramin administration into the respiratory tract in an aerosolized form could be even
454 considered, although this requires new safety studies.

455 In conclusion, our preclinical study shows that suramin inhibits SARS-CoV-2 replication in cell culture,
456 likely by preventing entry. Suramin also appears to prevent progression of SARS-CoV-2 infection in a
457 human airway epithelial cell culture model. This is only the first step towards evaluating whether
458 suramin treatment could provide any benefit to COVID-19 patients. Further studies should carefully
459 evaluate different formulations, routes of administration, pharmacokinetics, and possible adverse
460 effects in cell culture and *ex vivo* models. Ultimately, the clinical benefits of suramin for the treatment
461 of COVID-19 patients should be evaluated in carefully performed and properly controlled clinical trials.
462

463

464 **Acknowledgements**

465 The authors would like to thank Jessika Zevenhoven and Linda Boomaars-van der Zanden for technical
466 assistance and Anne van der Does for helpful discussions. Clarisse S. B. da Silva was supported by the
467 Coordination for the Improvement of Higher Education Personnel (CAPES) (Process nr.
468 88881.171440/2018-01), Ministry of Education, Brazil. Ying Wang was supported in part by a grant
469 from the China Scholarship Council. Part of this research was supported by the Leiden University Fund
470 (LUF), the Bontius Foundation and donations from the crowdfunding initiative "wake up to corona".

471 **References**

- 472 1. Lu H, Stratton CW, Tang YW. 2020. Outbreak of pneumonia of unknown etiology in Wuhan,
473 China: The mystery and the miracle. *J Med Virol* 92:401-402.
- 474 2. Zhou P, Yang XL, Wang XG, Hu B, Zhang L, Zhang W, Si HR, Zhu Y, Li B, Huang CL, Chen HD,
475 Chen J, Luo Y, Guo H, Jiang RD, Liu MQ, Chen Y, Shen XR, Wang X, Zheng XS, Zhao K, Chen QJ,
476 Deng F, Liu LL, Yan B, Zhan FX, Wang YY, Xiao GF, Shi ZL. 2020. A pneumonia outbreak
477 associated with a new coronavirus of probable bat origin. *Nature* 579:270-273.
- 478 3. Gorbalenya AE, Baker SC, Baric RS, de Groot RJ, Drosten C, Gulyaeva AA, Haagmans BL,
479 Lauber C, Leontovich AM, Neuman BW, Penzar D, Perlman S, Poon LLM, Samborskiy DV,
480 Sidorov IA, Sola I, Ziebuhr J, Coronaviridae Study Group of the International Committee on
481 Taxonomy of V. 2020. The species Severe acute respiratory syndrome-related coronavirus:
482 classifying 2019-nCoV and naming it SARS-CoV-2. *Nature Microbiology* 5:536-544.
- 483 4. WHO. 2020. World Health Organization, Coronavirus disease 2019 (COVID-19) Situation
484 Report 106.
- 485 5. Weiss SR, Navas-Martin S. 2005. Coronavirus pathogenesis and the emerging pathogen
486 severe acute respiratory syndrome coronavirus. *Microbiol Mol Biol Rev* 69:635-64.
- 487 6. Huang C, Wang Y, Li X, Ren L, Zhao J, Hu Y, Zhang L, Fan G, Xu J, Gu X, Cheng Z, Yu T, Xia J,
488 Wei Y, Wu W, Xie X, Yin W, Li H, Liu M, Xiao Y, Gao H, Guo L, Xie J, Wang G, Jiang R, Gao Z, Jin
489 Q, Wang J, Cao B. 2020. Clinical features of patients infected with 2019 novel coronavirus in
490 Wuhan, China. *The Lancet* 395:497-506.
- 491 7. Wang M, Cao R, Zhang L, Yang X, Liu J, Xu M, Shi Z, Hu Z, Zhong W, Xiao G. 2020. Remdesivir
492 and chloroquine effectively inhibit the recently emerged novel coronavirus (2019-nCoV) in
493 vitro. *Cell Res* 30:269-271.
- 494 8. NIAID. 2020. National Institute of Allergy and Infectious Diseases. Adaptive COVID-19
495 Treatment Trial (ACTT). ClinicalTrials.gov Identifier: NCT04280705.
- 496 9. Voogd TE, Vansterkenburg EL, Wilting J, Janssen LH. 1993. Recent research on the biological
497 activity of suramin. *Pharmacol Rev* 45:177-203.
- 498 10. Yahi N, Sabatier JM, Nickel P, Mabrouk K, Gonzalez-Scarano F, Fantini J. 1994. Suramin
499 inhibits binding of the V3 region of HIV-1 envelope glycoprotein gp120 to
500 galactosylceramide, the receptor for HIV-1 gp120 on human colon epithelial cells. *J Biol*
501 *Chem* 269:24349-53.
- 502 11. Garson JA, Lubach D, Passas J, Whitby K, Grant PR. 1999. Suramin blocks hepatitis C binding
503 to human hepatoma cells in vitro. *J Med Virol* 57:238-42.
- 504 12. Aguilar JS, Rice M, Wagner EK. 1999. The polysulfonated compound suramin blocks
505 adsorption and lateral diffusion of herpes simplex virus type-1 in vero cells. *Virology* 258:141-
506 51.
- 507 13. Albuлесcu IC, Kovacikova K, Tas A, Snijder EJ, van Hemert MJ. 2017. Suramin inhibits Zika
508 virus replication by interfering with virus attachment and release of infectious particles.
509 *Antiviral Res* 143:230-236.
- 510 14. Basavannacharya C, Vasudevan SG. 2014. Suramin inhibits helicase activity of NS3 protein of
511 dengue virus in a fluorescence-based high throughput assay format. *Biochem Biophys Res*
512 *Commun* 453:539-44.
- 513 15. Albuлесcu IC, van Hoolwerff M, Wolters LA, Bottaro E, Nastruzzi C, Yang SC, Tsay SC, Hwu JR,
514 Snijder EJ, van Hemert MJ. 2015. Suramin inhibits chikungunya virus replication through
515 multiple mechanisms. *Antiviral Res* 121:39-46.
- 516 16. Yoshikawa T, Hill TE, Yoshikawa N, Popov VL, Galindo CL, Garner HR, Peters CJ, Tseng C-TK.
517 2010. Dynamic innate immune responses of human bronchial epithelial cells to severe acute
518 respiratory syndrome-associated coronavirus infection. *PloS one* 5:e8729-e8729.
- 519 17. Kovacikova K, Morren BM, Tas A, Albuлесcu IC, van Rijswijk R, Jarhad DB, Shin YS, Jang MH,
520 Kim G, Lee HW, Jeong LS, Snijder EJ, van Hemert MJ. 2020. 6'- β -Fluoro-homoaristeromycin
521 and 6'-fluoro-homoneplanocin A are potent inhibitors of chikungunya virus replication

- 522 through their direct effect on the viral non-structural protein 1. doi:10.1128/AAC.02532-19
523 %J Antimicrobial Agents and Chemotherapy: AAC.02532-19.
- 524 18. Schrupf JA, Ninaber DK, van der Does AM, Hiemstra PS. 2020. TGF- β 1 Impairs Vitamin D-
525 Induced and Constitutive Airway Epithelial Host Defense Mechanisms. *Journal of innate*
526 *immunity* 12:74-89.
- 527 19. Amatngalim GD, Schrupf JA, Dishchekenian F, Mertens TCJ, Ninaber DK, van der Linden AC,
528 Pilette C, Taube C, Hiemstra PS, van der Does AM. 2018. Aberrant epithelial differentiation
529 by cigarette smoke dysregulates respiratory host defence. *51:1701009*.
- 530 20. Kovacicova K, Morren BM, Tas A, Albuлесcu IC, van Rijswijk R, Jarhad DB, Shin YS, Jang MH,
531 Kim G, Lee HW, Jeong LS, Snijder EJ, van Hemert MJ. 2020. 6'- β -Fluoro-Homoaristeromycin
532 and 6'-Fluoro-Homoneplanocin A Are Potent Inhibitors of Chikungunya Virus Replication
533 through Their Direct Effect on Viral Nonstructural Protein 1. *64:e02532-19*.
- 534 21. Corman VM, Landt O, Kaiser M, Molenkamp R, Meijer A, Chu DKW, Bleicker T, Brünink S,
535 Schneider J, Schmidt ML, Mulders DGJC, Haagmans BL, van der Veer B, van den Brink S,
536 Wijsman L, Goderski G, Romette J-L, Ellis J, Zambon M, Peiris M, Goossens H, Reusken C,
537 Koopmans MPG, Drosten C. 2020. Detection of 2019 novel coronavirus (2019-nCoV) by real-
538 time RT-PCR. *Euro surveillance : bulletin Europeen sur les maladies transmissibles =*
539 *European communicable disease bulletin* 25:2000045.
- 540 22. Scholte FEM, Tas A, Martina BEE, Cordioli P, Narayanan K, Makino S, Snijder EJ, van Hemert
541 MJ. 2013. Characterization of Synthetic Chikungunya Viruses Based on the Consensus
542 Sequence of Recent E1-226V Isolates. *PLOS ONE* 8:e71047.
- 543 23. Sheahan TP, Sims AC, Graham RL, Menachery VD, Gralinski LE, Case JB, Leist SR, Pirc K, Feng
544 JY, Trantcheva I, Bannister R, Park Y, Babusis D, Clarke MO, Mackman RL, Spahn JE, Palmiotti
545 CA, Siegel D, Ray AS, Cihlar T, Jordan R, Denison MR, Baric RS. 2017. Broad-spectrum
546 antiviral GS-5734 inhibits both epidemic and zoonotic coronaviruses. *Sci Transl Med* 9.
- 547 24. Sheahan TP, Sims AC, Zhou S, Graham RL, Pruijssers AJ, Agostini ML, Leist SR, Schafer A,
548 Dinno KH, 3rd, Stevens LJ, Chappell JD, Lu X, Hughes TM, George AS, Hill CS, Montgomery
549 SA, Brown AJ, Bluemling GR, Natchus MG, Saindane M, Kolykhalov AA, Painter G, Harcourt J,
550 Tamin A, Thornburg NJ, Swanstrom R, Denison MR, Baric RS. 2020. An orally bioavailable
551 broad-spectrum antiviral inhibits SARS-CoV-2 in human airway epithelial cell cultures and
552 multiple coronaviruses in mice. *Sci Transl Med* doi:10.1126/scitranslmed.abb5883.
- 553 25. Sims AC, Baric RS, Yount B, Burkett SE, Collins PL, Pickles RJ. 2005. Severe acute respiratory
554 syndrome coronavirus infection of human ciliated airway epithelia: role of ciliated cells in
555 viral spread in the conducting airways of the lungs. *J Virol* 79:15511-24.
- 556 26. Wang M, Cao R, Zhang L, Yang X, Liu J, Xu M, Shi Z, Hu Z, Zhong W, Xiao G. 2020. Remdesivir
557 and chloroquine effectively inhibit the recently emerged novel coronavirus (2019-nCoV) in
558 vitro. *Cell Research* 30:269-271.
- 559 27. Cao B, Wang Y, Wen D, Liu W, Wang J, Fan G, Ruan L, Song B, Cai Y, Wei M, Li X, Xia J, Chen
560 N, Xiang J, Yu T, Bai T, Xie X, Zhang L, Li C, Yuan Y, Chen H, Li H, Huang H, Tu S, Gong F, Liu Y,
561 Wei Y, Dong C, Zhou F, Gu X, Xu J, Liu Z, Zhang Y, Li H, Shang L, Wang K, Li K, Zhou X, Dong X,
562 Qu Z, Lu S, Hu X, Ruan S, Luo S, Wu J, Peng L, Cheng F, Pan L, Zou J, Jia C, et al. 2020. A Trial
563 of Lopinavir-Ritonavir in Adults Hospitalized with Severe Covid-19.
564 doi:10.1056/NEJMoa2001282.
- 565 28. Molina JM, Delaugerre C, Le Goff J, Mela-Lima B, Ponscarne D, Goldwirt L, de Castro N.
566 2020. No evidence of rapid antiviral clearance or clinical benefit with the combination of
567 hydroxychloroquine and azithromycin in patients with severe COVID-19 infection. *Médecine*
568 *et Maladies Infectieuses* doi:<https://doi.org/10.1016/j.medmal.2020.03.006>.
- 569 29. Tan CW, Sam IC, Chong WL, Lee VS, Chan YF. 2017. Polysulfonate suramin inhibits Zika virus
570 infection. *Antiviral Research* 143:186-194.

- 571 30. Chen Y, Maguire T, Hileman RE, Fromm JR, Esko JD, Linhardt RJ, Marks RM. 1997. Dengue
572 virus infectivity depends on envelope protein binding to target cell heparan sulfate. *Nature*
573 *Medicine* 3:866-871.
- 574 31. De Clercq E. 1979. Suramin: A potent inhibitor of the reverse transcriptase of RNA tumor
575 viruses. *Cancer Letters* 8:9-22.
- 576 32. Kaplan LD, Wolfe PR, Volberding PA, Feorino P, Abrams DI, Levy JA, Wong R, Kaufman L,
577 Gottlieb MS. 1987. Lack of response to suramin in patients with AIDS and AIDS-related
578 complex. *The American Journal of Medicine* 82:615-620.
- 579 33. Wiedemar N, Hauser DA, Mäser P. 2020. 100 Years of Suramin. 64:e01168-19.
- 580 34. Ho Y-J, Wang Y-M, Lu J-w, Wu T-Y, Lin L-I, Kuo S-C, Lin C-C. 2015. Suramin Inhibits
581 Chikungunya Virus Entry and Transmission. *PLOS ONE* 10:e0133511.
- 582 35. Hiemstra PS, Tetley TD, Janes SM. 2019. Airway and alveolar epithelial cells in culture.
583 54:1900742.
- 584 36. Fulcher ML, Randell SH. 2013. Human Nasal and Tracheo-Bronchial Respiratory Epithelial Cell
585 Culture, p 109-121. *In* Randell SH, Fulcher ML (ed), *Epithelial Cell Culture Protocols: Second*
586 *Edition* doi:10.1007/978-1-62703-125-7_8. Humana Press, Totowa, NJ.
- 587 37. Hoffmann M, Kleine-Weber H, Schroeder S, Krüger N, Herrler T, Erichsen S, Schiergens TS,
588 Herrler G, Wu N-H, Nitsche A, Müller MA, Drosten C, Pöhlmann S. 2020. SARS-CoV-2 Cell
589 Entry Depends on ACE2 and TMPRSS2 and Is Blocked by a Clinically Proven Protease
590 Inhibitor. *Cell* 181:271-280.e8.
- 591 38. Menachery VD, Yount BL, Debbink K, Agnihothram S, Gralinski LE, Plante JA, Graham RL,
592 Scobey T, Ge X-Y, Donaldson EF, Randell SH, Lanzavecchia A, Marasco WA, Shi Z-L, Baric RS.
593 2015. A SARS-like cluster of circulating bat coronaviruses shows potential for human
594 emergence. *Nature Medicine* 21:1508-1513.
- 595 39. Lescure F-X, Bouadma L, Nguyen D, Parisey M, Wicky P-H, Behillil S, Gaymard A,
596 Bouscambert-Duchamp M, Donati F, Le Hingrat Q, Enouf V, Houhou-Fidouh N, Valette M,
597 Mailles A, Lucet J-C, Mentre F, Duval X, Descamps D, Malvy D, Timsit J-F, Lina B, van-der-
598 Werf S, Yazdanpanah Y. 2020. Clinical and virological data of the first cases of COVID-19 in
599 Europe: a case series. *The Lancet Infectious Diseases* doi:[https://doi.org/10.1016/S1473-3099\(20\)30200-0](https://doi.org/10.1016/S1473-3099(20)30200-0).
- 600
- 601 40. Rockx B, Kuiken T, Herfst S, Bestebroer T, Lamers MM, Oude Munnink BB, de Meulder D, van
602 Amerongen G, van den Brand J, Okba NMA, Schipper D, van Run P, Leijten L, Sikkema R,
603 Verschoor E, Verstrepen B, Bogers W, Langermans J, Drosten C, Fentener van Vlissingen M,
604 Fouchier R, de Swart R, Koopmans M, Haagmans BL. 2020. Comparative pathogenesis of
605 COVID-19, MERS, and SARS in a nonhuman primate model. *Science (New York, NY)*
606 doi:10.1126/science.abb7314:eabb7314.
- 607 41. Wölfel R, Corman VM, Guggemos W, Seilmaier M, Zange S, Müller MA, Niemeyer D, Jones
608 TC, Vollmar P, Rothe C, Hoelscher M, Bleicker T, Brünink S, Schneider J, Ehmann R,
609 Zwirgmaier K, Drosten C, Wendtner C. 2020. Virological assessment of hospitalized patients
610 with COVID-2019. *Nature* doi:10.1038/s41586-020-2196-x.

611

612